Atmospheric transfer of a radio-frequency clock signal with a diode laser

Jinsong Nie,[1,2] Lin Yang,[1] and Lingze Duan[1,*]

[1]Department of Physics, University of Alabama in Huntsville, Huntsville, Alabama 35899, USA

[2]State Key Laboratory of Pulsed Power Laser Technology, Hefei, Anhui 230037, China

*Corresponding author: lingze.duan@uah.edu

Received 30 July 2012; revised 22 October 2012; accepted 29 October 2012;
posted 30 October 2012 (Doc. ID 173449); published 30 November 2012

Remote transfer of a radio-frequency clock signal over a 60 m open atmospheric link has been experimentally investigated using a diode laser as the clock carrier. Phase-noise spectra and Allan deviations are both measured to characterize the excess clock instability incurred during the transfer process. Different detection schemes are used to assess the contributions from different noise sources. With an 80 MHz clock frequency, the total root-mean-square noise amplitude is measured to be about 5×10^{-3} rad, with fractional frequency instability on the order of 1×10^{-10} at 1 s. The majority of this excess noise is attributed to the transmitter noise, with the amplitude fluctuations of the diode laser identified as the main source. The excess phase noise caused by air turbulence is at the level of 10^{-4} rad under the current experimental conditions. Our finding suggests that suppressing the transmitter noise is critical for improving the clock-transfer fidelity.

OCIS codes: 120.0120, 010.3310, 140.2020.

1. Introduction

Over the last few years, considerable research attention has been given to the study of laser-based remote transfer of timing references [1–8]. While much of the prior work has focused on highly stable distribution of microwave clock signals via fiber links [1–4], there is a growing interest recently in exploring laser-based free-space timing transfer [5–8]. This is motivated by the projected need for high-fidelity optical links in the future space-terrestrial networks [9] and alternative navigating schemes independent of the global positioning system [10]. Notably, Sprenger *et al.* have studied the frequency stability of both optical-frequency and radio-frequency (RF) clock signals after 100 m atmospheric transmission [5]. Djerroud *et al.* have demonstrated a 5 km coherent optical link by transmitting a narrow-linewidth laser beam through turbulent atmosphere [6]. Finally, Gollapalli and Duan have demonstrated atmospheric transfer of both RF and optical clock signals over 60 m using a pulsed laser [7,8].

In general, transferring an RF clock signal suffers higher fractional instability than transferring an optical signal. This is due to the higher clock frequency of the latter scheme [11]. On the other hand, since the primary purpose of clock transfer is to synchronize local atomic clocks operating at the RF or microwave frequencies, transferring an optical reference signal would require every user to be able to downshift the reference clock from the optical-frequency range to the RF range, which adds substantial complexity to the user systems. From this point of view, direct delivery of RF clocks is practically more feasible.

The simplest approach to optically transfer an RF clock signal is by sending an amplitude-modulated (AM) cw laser through a delivery channel (e.g., a fiber or free-space link) and then recovering the clock signal at the user site with a photodetector [11]. Compared to other schemes, such as femtosecond

1559-128X/12/348190-05$15.00/0

laser-based clock transfer [7,8], using cw lasers is simple and low-cost. In particular, diode lasers offer superior compactness and seamless integration with modulators. Although extensively studied in fiber-optic systems [2,4], diode lasers have not been widely used in free-space clock transfer. The only prior work, to the best of our knowledge, is reported by Sprenger *et al.* [5], who measured the frequency stability of an 80 MHz clock, coded on a diode laser via direct current modulation, upon 100 m atmospheric transmission. Their work, however, gave only an upper bound of the transmission-induced instability due to the relatively large system noise. In addition, no phase-noise measurement was reported, leaving the short-term transfer stability uncharacterized. Given the application potential of diode laser-based atmospheric clock transfer, a more precise characterization of this basic technique is hence necessary.

Here we present the data from our recent rooftop experiments that aim to take an in-depth look at the clock degradation in diode laser-based atmospheric RF-clock transfer. We use an AM scheme similar to that used in [5]. But since the focus of this research is to evaluate the excess clock instability incurred by the transfer process, we derive the error signals through differential detection between the original clock and the transmitted clock. In addition, instead of directly modulating the laser current, we introduce an intensity modulator, which is less prone to causing laser instability. With these changes, we have been able to characterize the clock degradation in both the frequency domain (via phase-noise spectra) and the time domain (via the Allan deviation of the clock frequency). Moreover, we have applied two different detection configurations in our experiments to discriminate the excess noise from different sources. This allows us to assess the impact of various mechanisms of instability, which may prove to be valuable information for actual system design.

The paper is organized as follows. In Section 2, we will give a brief overview of the various noise sources involved in a laser-based RF-clock transfer system. That will be followed by a recap of the simple clock-transfer test, in which we simulate the actual clock transmission and recovery process with a single photodetector (1PD) used on the user side. Then in Section 4, we will describe a modified scheme in which a second photodetector is added to the local side to help remove the transmitter noise from the measurement. Such a two-photodetector (2PD) configuration allows us to make a better assessment of the instability caused by atmospheric turbulence. Finally, in Section 5, we will compare the data from the two configurations and draw conclusions.

2. Sources of Excess Noise

To deliver an RF-timing signal from a local reference to a remote user via an optical carrier, the simplest scheme involves (i) loading the clock signal onto the carrier (modulation), (ii) delivering the carrier to the user via an optical link (transmission), and (iii) extracting the clock signal from the carrier (recovery). In actual systems, all three steps degrade the original clock by adding excess noise into it.

On the local side, the amplitude noise of the optical carrier, primarily due to the instability of the laser and the optical amplifiers, degrades the quality of the amplitude modulation. The AM modulator adds random distortions to the clock signal because of its internal fluctuations. The transmitter electronics may also introduce excess noise. Altogether, these noise sources combine to produce what we refer to as the transmitter noise. Note that the instability of the local reference clock is not included here as our study focuses only on the excess noise and the differential detection scheme removes the reference-clock fluctuations from the measurement. For atmospheric clock transfer, the clock instability incurred during transmission is mainly caused by air turbulence. Turbulence induces fluctuations of the refractive index, which directly lead to excess phase noise in the recovered clock. Turbulence can also cause beam wander and speckle [12], which create intensity fluctuations on the receiver. In addition, beam scattering in the atmosphere and mechanical vibrations of the transmission optics may contribute to the transmission noise as well. Finally, on the user side, the photodetector adds detector noise, such as shot noise and thermal noise, to the recovered clock signal. The intensity fluctuations of the laser beam can also be converted into phase fluctuations of the clock through power-to-phase coupling [13]. In addition, the receiver electronics, mainly RF amplifiers, also introduce electronic noise. We shall collectively call these noises the receiver noise. Overall, when a user recovers the clock signal, he has no way to distinguish the excess fluctuations from the original clock instability. Therefore, all the aforementioned noises have to be taken into account when evaluating the fidelity of a clock-transfer system.

3. 1PD Configuration

Our clock transmission link is located 20 m above the ground on the roof of a laboratory building on the campus of the University of Alabama in Huntsville. A beam reflector is mounted on a sturdy tripod, which is anchored on the rooftop platform. The laser beam is launched from an astronomical observatory 30 m away via a fiber collimator. The reflector sends the beam back to the observatory to form a 60 m transmission link in open atmosphere. Figure 1(a) shows a schematic of the experimental setup. The optical carrier is provided by a single-frequency external-cavity semiconductor laser (Covega SFL1550S) centered at 1550 nm with a linewidth of about 200 kHz and an output power of 20 mW. An 80 MHz clock signal, generated by a crystal-controlled RF driver, is coded onto the carrier via a zero-chirp fiber-coupled intensity modulator (Thorlabs LN56S). The modulated laser beam is amplified by a commercial erbium-doped fiber amplifier (EDFA) to 40 mW before being launched into the free-space transmission link. The returning

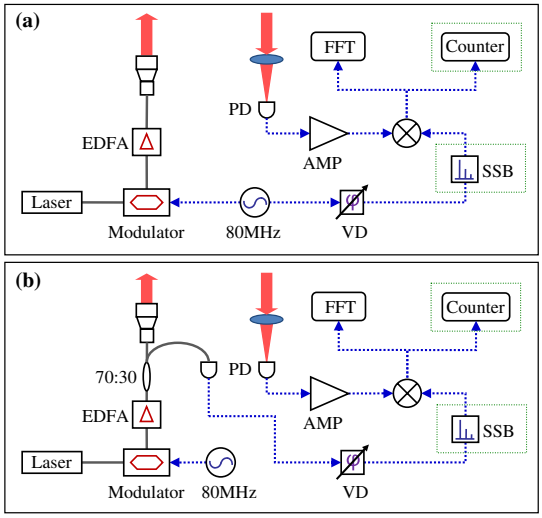

Fig. 1. (Color online) Schematics of the experimental systems for (a) 1PD configuration and (b) 2PD configuration. The dotted-line-enclosed parts are inserted when measuring Allan deviations. AMP, microwave amplifiers; PD, photodetectors; SSB, single sideband modulator; VD, variable delay.

beam of about 5 mW is collected by a large-aperture receiving system and then tightly focused onto a high-speed photodiode. The same receiving system has been used previously in a study of atmospheric clock transfer based on a femtosecond frequency comb, and has proved to be effective in minimizing the power fluctuation caused by beam wander and speckle [7]. The recovered clock signal is compared with a reference signal, which is derived directly from the RF driver, on a double-balanced mixer. With low-pass filtering, the mixer functions as a differential detector. In the phase-noise measurement, the reference clock passes through an adjustable delay line to gain a proper phase before it beats the transmitted clock in quadrature. The generated baseband signal is then frequency analyzed by a fast Fourier transform (FFT) analyzer (SRS SR785). In the frequency-stability measurement, the reference clock first gains a 1.4 MHz frequency shift at a single-sideband modulator (SSBM) and then mixes with the transmitted clock. This leads to a 1.4 MHz beat note, which is then measured with a frequency counter (SRS SR620) to determine its stability.

The experiment has been conducted under low-wind conditions with the wind speed generally below 2 m/s to avoid strong signal fading or structural vibration. A typical single-sideband (SSB) phase-noise spectrum between 1 Hz and 100 kHz (solid trace) is shown in Fig. 2. The phase noise at 1 Hz is about −60 dBc/Hz. As the frequency increases, the phase noise declines at a slope of approximately f^{-2}, indicating the general behavior of a white frequency modulation [14]. The spiky features within the range of 100 Hz–10 kHz are attributed to interference from the power circuits as discussed in the next section. Allan deviations have been measured to evaluate the clock-frequency stability, and the result is shown

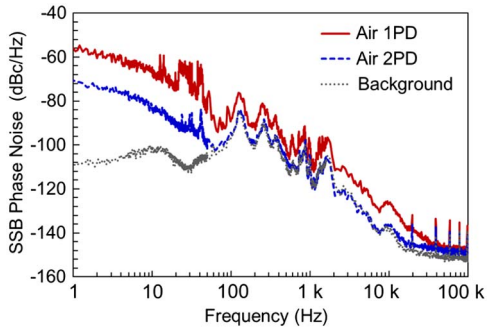

Fig. 2. (Color online) SSB phase-noise spectra of the transmitted clock signals with the 1PD and the 2PD configurations, along with the background noise spectrum.

in Fig. 3 (square). The fractional frequency instability of the transmitted clock is about 1×10^{-10} at 1 s, and the Allan deviation declines with the averaging time at approximately $\tau^{-1/2}$, both facts similar to the previous report [5]. The $\tau^{-1/2}$ dependence indicates that the frequency instability is likely due to white frequency modulation [14], which agrees with the phase-noise observation.

It should be noted that the excess noise measured with the 1PD configuration includes contributions from all the noise sources mentioned in Section 2. It is a realistic estimate of the excess instability a user can expect from such a clock-transfer scheme. However, when making comparisons with other atmospheric RF-clock distribution methods, one must keep in mind that the fractional instability is inversely proportional to the clock frequency. Our current test equipment limits the clock frequency to 80 MHz, which is very low for a technique based on optical carriers. In practice, the impact of these excess noises can be considerably reduced by simply raising the clock frequency.

4. 2PD Configuration

Although the clock instability measured with the 1PD configuration provides a realistic estimate of the transfer fidelity, it offers little information about the relative impact of each individual noise mechanism. In particular, it would be interesting to find out

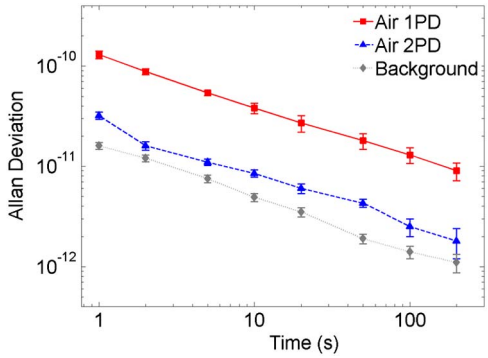

Fig. 3. (Color online) Allan deviations of the transmitted clock, measured with both the 1PD and the 2PD configurations, and the background noise, measured with the 2PD configuration.

the relative contributions of the transmitter noise, the receiver noise, and the noise induced by air turbulence. This is an important question in practice because it determines which aspect is limiting the performance of the scheme. To answer that question, we slightly modified the experimental configuration to add some discrimination to the effects from different noise sources. As shown in Fig. 1(b), a second photodetector is inserted right before the fiber collimator, where a 70∶30 coupler routes a small portion of the modulated laser beam directly to the detector. The extracted clock signal is then used as the reference signal in the new configuration. With this configuration, all the noise added to the clock signal before the fiber coupler, i.e., the transmitter noise, becomes common mode, and is therefore removed by the differential detector. The turbulence-induced noise and the receiver noise, however, remain to be detectable.

We have performed the same phase-noise measurement using the 2PD configuration, and the result is shown in Fig. 2 (dashed trace). The trace possesses similar features to those from the 1PD measurement but stays about 10 dB below the solid trace up to 30 kHz, where the white noise floor of the FFT analyzer begins to dominate. The Allan deviation measurement, as shown in Fig. 3 (triangles), indicates a uniform reduction (~6 dB) of instability across the time scales of the measurement with a similar $\tau^{-1/2}$ behavior.

In order to further distinguish the turbulence-induced noise from the receiver noise and verify the proper operation of the transmission link, we have also made a background measurement by rerouting the collimated beam directly into the receiving system without sending it to the outdoor link. The corresponding phase-noise spectrum and Allan deviations, which are now due only to the receiver noise (including also a small contribution from the noise of the measurement instruments such as the FFT analyzer), are shown in Fig. 2 (dotted trace) and Fig. 3 (diamonds), respectively. Comparing the two phase-noise spectra measured with the 2PD configuration, i.e., the dashed trace versus the dotted trace, it is obvious that the turbulence-induced phase noise dominates the noise spectrum at low frequencies (e.g., below 100 Hz), whereas the noise at higher frequencies is mainly due to the system background. Moreover, all three spectra in Fig. 2 share similar features above 100 Hz, suggesting that these features are likely due to fluctuations in the power circuits, which are common for all three curves. Meanwhile, the fractional instability of the background signal is about 3 dB below that of the 2PD transmitted clock and 10 dB below that of the 1PD transmitted clock.

5. Discussion and Conclusion

Figures 2 and 3 provide two different views of the clock instability, i.e., a frequency-domain description of the short-term instability (Fig. 2) and a time-domain description of the long-term instability (Fig. 3). Sometimes, however, a direct account of the noise magnitude in time domain is desired to quantify the relative contributions of the various noise sources. This can be done by assessing the root-mean-square (RMS) noise amplitude, which can be computed from the phase-noise spectra by integrating the spectral curves over a certain bandwidth [11]. Figure 4 shows the RMS phase-noise amplitudes for the three curves in Fig. 2, integrated from 100 kHz down to 1 Hz. The relative scales of these three curves offer useful insight into the relative contributions of various noise sources. For example, the solid curve understandably stays well above the other two curves over almost the entire frequency range as the transmitted clock signal in the 1PD configuration carries the contributions from all noise sources. Its difference from the dashed curve, which only includes the contributions from the turbulence and the receiver, allows us to estimate the relative contribution of the transmitter noise. On the other hand, the difference between the dashed curve and the dotted curve accounts for the excess noise induced by the air turbulence.

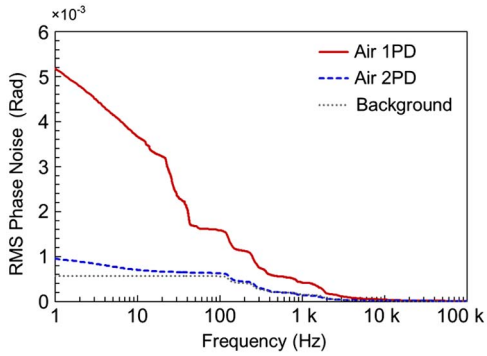

Fig. 4. (Color online) RMS phase-noise amplitudes computed by integrating the three curves in Fig. 2 from 100 kHz to 1 Hz. The differences between the three traces embody the relative contributions of the different noise sources.

When integrated over the entire frequency span of the measurement (values at 1 Hz in Fig. 4), the RMS noise amplitudes for the three cases are 5.2×10^{-3} rad, 9.5×10^{-4} rad, and 5.7×10^{-4} rad, respectively. One would immediately notice that the relative scales of the RMS phase noise of these three traces are consistent with the relative scales of the Allan deviation measurement. For example, the RMS phase noise of the solid trace is about five times greater than that of the dashed trace and 10 times greater than that of the dotted trace, agreeing well with the result shown in Fig. 3. Also, the noise amplitudes due to the transmitter, the air turbulence, and the receiver are found to be 5.1×10^{-3} rad, 7.6×10^{-4} rad, and 5.7×10^{-4} rad, respectively. Of particular interest is the turbulence-induced noise, which is subject to comparisons with similar results obtained with a femtosecond frequency comb [7]. The RMS timing jitter has been determined in [7] to be about 0.5–2 ps using the same atmospheric link.

With an 80 MHz clock frequency, this corresponds to a RMS phase noise $2.5 \times 10^{-4} - 1.0 \times 10^{-3}$ rad, which is in agreement with the 7.6×10^{-4} rad measured with the diode laser.

Meanwhile, it is quite interesting to see that the transmitter noise is almost a factor of 7 greater than the turbulence-induced noise in the current experiment. This is partly because the atmospheric propagation distance is very short and we chose to collect the data under low-wind conditions. For longer transmission distances, the contribution from the turbulence will scale up [15] and may eventually become the dominant factor. However, it is still somewhat surprising to realize that transmitter noise plays such a critical role in the overall transfer quality. Since the electronics in the transmitter are about the same as those used in the receiver, and the receiver noise is an order of magnitude lower, the large transmitter noise is likely caused by the intensity fluctuations of the diode laser and the EDFA. To further distinguish their contributions in the overall transmitter noise, we performed the background measurement with and without the EDFA and found that the RMS phase noise due to the EDFA is an order of magnitude lower than that due to the diode laser. This suggests that, in the design of practical systems, laser amplitude stabilization should be seriously considered.

In conclusion, we have made an in-depth study of atmospheric RF-clock transfer using a diode laser. The excess clock instability incurred during the transfer process is characterized by both phase-noise spectra and Allan deviations under typical low-wind conditions. Two detection schemes are used to isolate the effects of different noise sources. The overall fractional frequency instability for a 60 m transmission in open atmosphere has been found to be on the order of one part per 10^{10} at 1 s with an 80 MHz clock frequency. The corresponding RMS phase-noise amplitude is approximately 5.1×10^{-3} rad. The majority of this excess noise, however, is found to be due to the transmitter noise, with its main contribution coming from the amplitude noise of the diode laser. The excess phase noise caused by air turbulence has an RMS amplitude of about 7.6×10^{-4} rad under the current transmission distance and weather conditions. Such a level is well below the transmitter noise. Even when the turbulence-induced noise scales up at longer transmission distances, the significant impact of the laser and amplifier noise is still noteworthy. Amplitude-stabilized laser sources are highly recommended for a future clock-transfer system design based on diode lasers. Finally, it should be noted here that the present work is in no way a complete survey of the pertinent clock-transfer scheme under various weather conditions. Rather, it seeks to learn some of the general characteristics of the technique under typical operating conditions.

This work is supported by the China Scholarship Council and the University of Alabama in Huntsville. We thank the UAH Center for Applied Optics, especially Ted Rodgers and Patrick Reardon, for provision of the experimental space.

References

1. K. W. Holman, D. D. Hudson, J. Ye, and D. J. Jones, "Remote transfer of a high-stability and ultralow-jitter timing signal," Opt. Lett. **30**, 1225–1227 (2005).
2. M. Kumagai, M. Fujieda, S. Nagano, and M. Hosokawa, "Stable radio frequency transfer in 114 km urban optical fiber link," Opt. Lett. **34**, 2949–2951 (2009).
3. G. Marra, H. S. Margolis, S. N. Lea, and P. Gill, "High-stability microwave frequency transfer by propagation of an optical frequency comb over 50 km of optical fiber," Opt. Lett. **35**, 1025–1027 (2010).
4. O. Lopez, A. Amy-Klein, M. Lours, C. Chardonnet, and G. Santarelli, "High-resolution microwave frequency dissemination on an 86 km urban optical link," Appl. Phys. B **98**, 723–727 (2010).
5. B. Sprenger, J. Zhang, Z. H. Lu, and L. J. Wang, "Atmospheric transfer of optical and radio frequency clock signals," Opt. Lett. **34**, 965–967 (2009).
6. K. Djerroud, O. Acef, A. Clairon, P. Lemonde, C. N. Man, E. Samain, and P. Wolf, "Coherent optical link through the turbulent atmosphere," Opt. Lett. **35**, 1479–1481 (2010).
7. R. P. Gollapalli and L. Z. Duan, "Atmospheric timing transfer using a femtosecond frequency comb," IEEE Photon. J. **2**, 904–910 (2010).
8. R. P. Gollapalli and L. Z. Duan, "Multiheterodyne characterization of excess phase noise in atmospheric transfer of a femtosecond-laser frequency comb," J. Lightwave Technol. **29**, 3401–3407 (2011).
9. V. W. S. Chan, "Free-space optical communications," J. Lightwave Technol. **24**, 4750–4762 (2006).
10. F. Pappalardi, S. J. Dunham, M. E. LeBlang, T. E. Jones, J. Bangert, and G. Kaplan, "Alternatives to GPS," in *Proceedings of OCEANS 2001, MTS/IEEE Conference and Exhibition* (IEEE, 2001), pp. 1452–1459.
11. S. M. Foreman, K. W. Holman, D. D. Hudson, D. J. Jones, and J. Ye, "Remote transfer of ultrastable frequency references via fiber networks," Rev. Sci. Instrum. **78**, 021101 (2007).
12. L. C. Andrews and R. L. Phillips, *Laser Beam Propagation Through Random Media*, 2nd ed. (SPIE, 2005).
13. E. N. Ivanov, S. A. Diddams, and L. Hollberg, "Analysis of noise mechanisms limiting the frequency stability of microwave signals generated with a femtosecond laser," IEEE J. Sel. Topics Quantum Electron. **9**, 1059–1065 (2003).
14. J. Levine, "Introduction to time and frequency metrology," Rev. Sci. Instrum. **70**, 2567–2596 (1999).
15. A. Alatawi, R. P. Gollapalli, and L. Z. Duan, "Radio-frequency clock delivery via free-space frequency comb transmission," Opt. Lett. **34**, 3346–3348 (2009).